J. Appl. Comput. Mech., 5(4) (2019) 791-803
DOI: 10.22055/JACM.2019.28147.1456

ISSN: 2383-4536
jacm.scu.ac.ir

M&MoCS

Shahid Chamran University of Ahvaz

Journal of Applied and Computational Mechanics

Research Paper

Chemical Reaction Effects on Bio-Convection Nanofluid flow between two Parallel Plates in Rotating System with Variable Viscosity: A Numerical Study

Nainaru Tarakaramu[1], P.V. Satya Narayana[2]

[1] Department of Mathematics, SAS, VIT, Vellore-632014, T.N, India, Email: nainaru.tarakaramu@vit.ac.in
[2] Department of Mathematics, SAS, VIT, Vellore-632014, T.N, India, Email: psatya@vit.ac.in

Received January 07 2019; Revised February 21 2019; Accepted for publication February 26 2019.
Corresponding author: P.V. Satya Narayana, psatya@vit.ac.in

Abstract. In the present work, a mathematical model is developed and analyzed to study the influence of nanoparticle concentration through Brownian motion and thermophoresis diffusion. The governing system of PDEs is transformed into a coupled non-linear ODEs by using suitable variables. The converted equations are then solved by using robust shooting method with the help of MATLAB (bvp4c). The impacts of dynamic parameters on the flow, energy and concentration are discussed graphically. It is noticed that the mass transfer rate in case of regular fluid is lower than that of nanofluid and the axial velocity converges to the boundary very fast in case of temperature dependent viscosity in comparison with the regular viscous fluid.

Keywords: Bio-convection, Magnetohydrodynamic, Thermal Radiation, Chemical Reaction, Variable Viscosity, Nanofluid.

1. Introduction

The nanofluid [1] is an innovative type of fluid containing small sized particles in the ordinary fluid. The thermal conductivity of the convectional fluids (like water, oil, and ethylene glycol) has been increased by suspending nano-particles in base fluids. It has more applications in industrial and engineering processes like chemical processes, power generation, manufacturing and transportation. The fluid motion of macroscopic convective flow caused by the density is slightly higher than water, which is called “bio-convection” [2-3]. It is useful in fuel cell technology, bio-reactors, bio-diesel fuels, bio-microsystems and gas bearing sedimentary, etc. The benefits of adding motile microorganisms to nanoparticles are to enhance the mass transfer and improve the stability of nanofluid. Different bio-convection nanofluid models were studied on the basis different types of microorganisms and the directional motion mechanism of the fluid. Chidress et al. [4] developed the simple modal for pattern formation in layered suspension of swimming micro-organism. They concluded that, the maximum growth rate determined a preferred pattern size explicitly in terms of U and D. Hill et al. [5] investigated the influence of bio-convection patterns in a gyrotactic microorganisms with a finite depth in the layers. They found that the existence of oscillatory modes were driven by the gyrotactic response of the micro-organisms at the rigid boundaries. Kuznetsov et al. [6] proposed an oscillatory convection in a water based nanofluids containing oxytactic microorganisms, nanoparticles. This study analyzed that the destabilizing effect of microorganisms was due to the higher suspension of concentration of the fluid. Recent publications [7-20] explored the significant interest of nanofluids in distinct types of microsystems.

Bio-convective flows in the presence of MHD have several applications in the fields of polymer expulsion, treatment of some arterial diseases and hyperthermia, drawing of copper wires, and reduction of blood during surgeries, etc. Naseem et al. [21] explored the study of MHD bio-convection non-Newtonian nanofluid flow due to a sheet stretching and concluded that, the motile density profile reduced for higher Péclet and bioconvection Lewis number. Chakraborty et al. [22] studied the effect

Published online: May 10 2019

of external magnetic field on gyrotactic microorganisms and derived a conclusion that, the self-moving microorganism flux raised with increasing surface convection parameter and opposite result with Péclet number. Alsaedi et al. [23] presented the viscous dissipation, joule heating effects on MHD bio-convection flow of nanofluid containing gyrotactic microorganisms past a porous wedge. Recently, many researchers [24-30] investigated the influence of MHD on different fluid flows in various geometrical configurations.

Chemical reaction has one of the significant roles in bio and chemical manufacturing claims such as food processing, manufacturing of ceramics and drying, etc. Khan et al. [31] devoted the magnetohydrodynamic Williamson nanofluid with chemical reaction and it is found that, the temperature profile raised for large values of thermophoresis. The impact of heat sou rce on magnetohydrodynamic viscoelastic fluid flow through a porous channel was considered by Devika et al. [32]. Thi s study reveals that, the concentration of the fluid decreases due to the presence of chemical reaction. This is due to the consumption of chemical species. Jena et al. [33] explored the impact of heat and mass transfer on magnetohydrodynamic Jeffrey fluid through a stretching sheet and they concluded that the elasticity of the fluid reduced the temperature near the bounding area. Javaid et al. [34] studied the heat transfer of magnetohydrodynamic power law fluid through porous sheet. Satya Narayana et al. [35] inspected the influence of heat source and chemical reaction on magnetohydrodynamic oscillating flow in an asymmetric channel. Hayat et al. [36] discussed the chemical reaction and thermal radiation effects on MHD convective flow owing to a curved surface. Very few investigators [37-44] discussed the heat and mass transfer on magnetohydrodynamic flow with bio-convection in a rotating system.

The literature reveals that the study on MHD flow with bio-convection nanofluid containing gyrotactic microorganisms in a rotating system with chemical reaction is scant. These type of models find the valuable applications in medical and engineering fields like, modeling oil, gas bearing sedimentary, bio-micro systems. So, the main aim of this effort is to apply magnetic field in two phase rotating system for bio-convection nanofluid flow model with chemical reaction. The non-linear coupled equations are solved numerically by utilizing R-K-F procedure. Graphically results are displayed to study the various physical parameters like bio-convection, Péclet number, magnetic field parameter and chemical reaction parameters on the flow fields. Also, the results are in good agreement with the outcomes available in the literature and results of this study are new and original.

2. Mathematical Formulation

The 3D flow of an incompressible, MHD bio-convection nanofluid between two horizontal parallel plates rotating about the y-axis with uniform angular velocity Ω is considered in this model as shown in Fig.1. A Cartesian coordinate system is chosen as follows: two pates are located at $y = 0$ and $y = h$, where plates are along the x-axis direction; z-axis is perpendicular to the xy -plane and the system is rotating about y-axis. The lower plate is stretched linearly by two equal and opposite forces so that the point (0,0,0) remains unaltered. The induced magnetic field and electric field are assumed to be neglected. Also, assume that suspended nanoparticles do not change the swimming direction and velocity of the motile microorganisms. Under these considerations, the governing equations expressing the conservation of the mass, momentum, energy, nanoparticles volume fraction and motile microorganisms are: [see ref. 25, 37, 45-49],

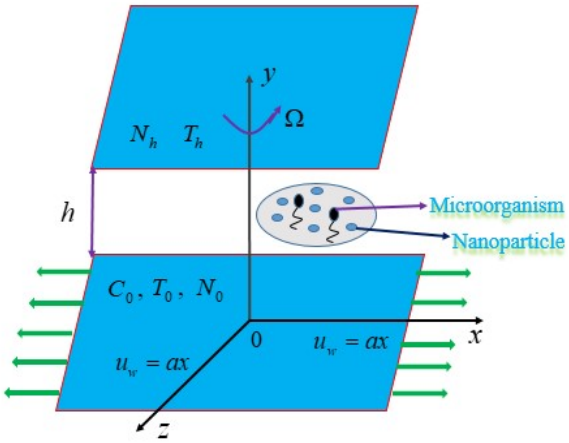

Fig. 1. The physical model of the problem

$$\frac{\partial A}{\partial x}+\frac{\partial B}{\partial y}+\frac{\partial C}{\partial z}=0 \tag{1}$$

$$A\frac{\partial A}{\partial x}+B\frac{\partial B}{\partial y}+2\Omega C=-\frac{1}{\rho_f}\frac{\partial p}{\partial x}+\frac{1}{\rho_f}\frac{\partial}{\partial y}\left(\mu\frac{\partial A}{\partial y}\right)-\frac{\sigma H_0^2}{\rho_f}A \tag{2}$$

$$A\frac{\partial B}{\partial x}+B\frac{\partial B}{\partial y}=-\frac{1}{\rho_f}\frac{\partial p}{\partial y}+\frac{1}{\rho_f}\frac{\partial}{\partial y}\left(\mu\frac{\partial B}{\partial y}\right) \tag{3}$$

$$A\frac{\partial C}{\partial x}+B\frac{\partial C}{\partial y}-2\Omega A=\frac{1}{\rho_f}\frac{\partial}{\partial y}\left(\mu\frac{\partial C}{\partial y}\right)-\frac{\sigma H_0^2}{\rho_f}C \tag{4}$$

$$\begin{aligned}A\frac{\partial\Theta}{\partial x}+B\frac{\partial\Theta}{\partial y}+C\frac{\partial\Theta}{\partial z}&=\frac{k}{\left(\rho c_p\right)_f}\left(\frac{\partial^2\Theta}{\partial x^2}+\frac{\partial^2\Theta}{\partial y^2}+\frac{\partial^2\Theta}{\partial z^2}\right)\\&+\tau\left\{D_0\left(\frac{\partial\Theta}{\partial x}\frac{\partial\Psi}{\partial x}+\frac{\partial\Theta}{\partial y}\frac{\partial\psi}{\partial y}+\frac{\partial\Theta}{\partial z}\frac{\partial\psi}{\partial z}\right)+\left(\frac{D_\Theta}{\Theta_0}\right)\left[\left(\frac{\partial\Theta}{\partial x}\right)^2+\left(\frac{\partial\Theta}{\partial y}\right)^2+\left(\frac{\partial\Theta}{\partial z}\right)^2\right]\right\}-\frac{1}{\left(\rho c_p\right)_f}\left(\frac{\partial q_r}{\partial y}\right)\end{aligned} \tag{5}$$

$$A\frac{\partial\Psi}{\partial x}+B\frac{\partial\Psi}{\partial y}+C\frac{\partial\Psi}{\partial z}=\left\{D_0\left(\frac{\partial^2\Psi}{\partial x^2}+\frac{\partial^2\Psi}{\partial y^2}+\frac{\partial^2\Psi}{\partial z^2}\right)+\left(\frac{D_\Theta}{\Theta_0}\right)\left[\left(\frac{\partial^2\Theta}{\partial x^2}+\frac{\partial^2\Theta}{\partial y^2}+\frac{\partial^2\Theta}{\partial z^2}\right)\right]\right\}-k\,\Psi \tag{6}$$

$$A\frac{\partial N}{\partial x}+B\frac{\partial N}{\partial y}+C\frac{\partial N}{\partial z}+\frac{bW_c}{C_0}\frac{\partial}{\partial y}\left\{S\frac{\partial C}{\partial y}\right\}=D_n\left(\frac{\partial^2 N}{\partial x^2}+\frac{\partial^2 N}{\partial y^2}+\frac{\partial^2 N}{\partial z^2}\right) \tag{7}$$

The appropriate boundary conditions are

$$\begin{aligned}&A=A_w(\mathrm{x})=\alpha x,\quad B=C=0,\quad \Theta=\Theta_0,\quad S=S_0,\quad \Psi=\Psi_0,\quad \text{at } y=0\\&A=B=C=0,\qquad \Theta=\Theta_h,\qquad S=S_h,\quad D_0\frac{\partial\Psi}{\partial y}+\frac{D_\Theta}{\Theta_0}\frac{\partial\Theta}{\partial y}=0,\quad \text{as } y\to h\end{aligned} \tag{8}$$

The fluid viscosity is a temperature dependent function and is defined as $\mu=\mu_0 f(\Theta)$, where $f(\Theta)=\exp(-b(\Theta-\Theta_1))$ [see refs. 49-52], b is a dimension of $[\Theta]^{-1}$. Also the fluid viscosity (μ) is taken as the inverse function of temperature (Θ), $1/\mu=\left[1+\gamma(\Theta-\Theta_\infty)\right]/\mu_0=a(\Theta-\Theta_r)$, [see Refs. 53-54] where $a=\gamma/\mu_\infty$ and $\Theta_r=(\Theta_\infty-1)/\gamma$ are constants and their values depend on thermal properties of the fluid. Generally, if $a>0$ then it is called liquids such as water, oils and if $a<0$ then it is called gases such as air. In the present work the fluid viscosity is defined as $\mu=\mu_0\exp(-\lambda\theta(\eta))$ [see Ref. 40] where the subscript 0 indicate the reference state $\Theta=\Theta_0$ and λ indicates the viscosity variation parameter.

The radiative heat flux q_r according to Rosseland approximation [55], is given by:

$$q_r=-\frac{4\sigma^*}{3K^*}\frac{\partial\Theta^4}{\partial y} \tag{9}$$

Assuming that the differences in temperature within the flow are sufficiently small such that Θ^4 can be expressed as a linear combination of the temperature about Θ_∞ as follows:

$$\Theta^4=\Theta_\infty^4+4\Theta_\infty^3(\Theta-\Theta_\infty)+6\Theta_\infty^2(\Theta-\Theta_\infty)^3+\ldots \tag{10}$$

Now by removing higher order terms beyond the first degree in $(\Theta-\Theta_\infty)$, one can get

$$\begin{aligned}\Theta^4&=4\Theta_\infty^3\Theta-3\Theta_\infty^4\\\frac{\partial q_r}{\partial y}&=-\frac{4\sigma^*\Theta^3}{3K^*}\frac{\partial^2\Theta}{\partial y^2}\end{aligned} \tag{11}$$

Substituting Eq. (11) into Eq. (5), one obtains:

$$\begin{aligned}A\frac{\partial\Theta}{\partial x}+B\frac{\partial\Theta}{\partial y}+C\frac{\partial\Theta}{\partial z}&=\frac{1}{\left(\rho c_p\right)_f}\left(k\left(\frac{\partial\Theta}{\partial x^2}+\frac{\partial^2\Theta}{\partial y^2}+\frac{\partial^2\Theta}{\partial z^2}\right)+\frac{16\sigma^*\Theta^3}{3k\,k^*}\frac{\partial^2\Theta}{\partial y^2}\right)\\&+\tau\left\{D_0\left(\frac{\partial\Theta}{\partial x}\frac{\partial\Psi}{\partial x}+\frac{\partial\Theta}{\partial y}\frac{\partial\Psi}{\partial y}+\frac{\partial\Theta}{\partial z}\frac{\partial\Psi}{\partial z}\right)+\left(\frac{D_\Theta}{\Theta_0}\right)\left[\left(\frac{\partial\Theta}{\partial x}\right)^2+\left(\frac{\partial\Theta}{\partial y}\right)^2+\left(\frac{\partial\Theta}{\partial z}\right)^2\right]\right\}\end{aligned} \tag{12}$$

The first order similarity variables are:

$$A = axf'(\eta),\quad B = -ahf(\eta),\quad C = axg(\eta)$$
$$\theta(\eta) = \frac{\Theta - \Theta_h}{\Theta_0 - \Theta_h},\quad \phi(\eta) = \frac{\Psi}{\Psi_0},\quad S(\eta) = \frac{N}{N_0},\quad \eta = \frac{y}{h} \tag{13}$$

In view of above variables, Eqs. (2) and (3) are transformed to:

$$-\frac{1}{\rho_f}\frac{\partial p}{\partial x} = a^2 x\left[(f')^2 - ff'' + \frac{2K_r}{R}g - \frac{1}{R}e^{-\lambda\theta}(f''' - \lambda\theta' f'') - \mathrm{M}f'\right] \tag{14}$$

$$-\frac{1}{\rho_f}\frac{\partial p}{\partial x} = a^2 h\left[ff' + \frac{1}{R}e^{-\lambda\theta}(f'' - \lambda\theta' f')\right] \tag{15}$$

Differentiating Eqs. (14), (15) with respect to y, *x,* respectively, we get:

$$e^{-\lambda\theta}\left[f^{iv} - \lambda\theta'' f'' - 2\lambda\theta' f''' + \lambda^2(\theta')^2 f''\right] - R(f'f'' - ff''' - f''M) - 2\mathrm{K}_r g' = 0 \tag{16}$$

and remaining Eq. (4)– (7) together with boundary conditions (8) generate the below four ODEs

$$e^{-\lambda\theta}\left[g'' - \lambda\theta' g'\right] - R(f'g - fg') + 2\mathrm{K}_r f' = 0 \tag{17}$$

$$(1+R_d)\theta'' + R\,\mathrm{Pr} f\theta' + \mathrm{N_b}\,\theta'\phi' + N_t(\theta')^2 = 0 \tag{18}$$

$$\phi'' + \frac{N_t}{N_b}\theta'' + R\,Le f\phi' + \gamma\phi R = 0 \tag{19}$$

$$S'' + R\,Sc f S' - Pe(\mathrm{S}'\phi' + \mathrm{S}\phi'') = 0 \tag{20}$$

The boundary conditions are

$$\begin{aligned} &f(0) = 0,\quad f'(0) = 1,\quad g(0) = 0,\quad \theta(0) = 1,\quad \phi(0) = 1,\quad S(0) = 1,\\ &f(1) = 0,\quad f'(1) = 0,\quad g(1) = 0,\quad \theta(1) = 0,\quad S(1) = \delta_s,\quad N_b\phi'(1) + N_t\theta'(1) = 0 \end{aligned} \tag{21}$$

The physical quantities on the lower plate are defined as

$$\begin{aligned} &\mathrm{Re}_x^{-1}C_f = \frac{-x}{h}f''(0),\quad \mathrm{Nu}_x = \frac{x}{h}\theta'(0),\quad Sh_x = \frac{x}{h}\phi''(0),\quad \mathrm{Q}_{nx} = \frac{x}{h}\mathrm{S}'(0),\\ &C_f = \frac{-\mu}{\rho_f(\mathrm{ax})^2}\left(\frac{\partial u}{\partial y}\right)_{y=0},\ Nu_x = \frac{-kx}{\mathrm{k}_0(\mathrm{T}_0 - \mathrm{T}_\mathrm{h})}\left(\frac{\partial T}{\partial y}\right)_{y=0},\ Sh_x = \frac{x}{C_0}\left(\frac{\partial C}{\partial y}\right)_{y=0},\ Q_{nx} = \frac{x}{N_0}\left(\frac{\partial N}{\partial y}\right)_{y=0} \end{aligned} \tag{22}$$

Here $\mathrm{Re}_x = \upsilon/(ax^2)$ refers to the local Reynolds number, Sh_x and the Nusselt number Nu_x along the stretching wall is defined as $Sh_x = -\phi'(\eta)$, $\mathrm{Nu}_x = -(1+R)\theta(0)$.

3. Results and Discussion

The transformed Eqs. (16) to (19) with boundary conditions (20) have been solved computationally by R-K-F algorithm along with shooting technique. The graphical results are shown in figures (2)-(11) for different parameters on the f, g, θ, ϕ and S profiles as well as Sh_x and Nu_x.

The impact of viscous variation parameter λ on f, g, ϕ, and S is demonstrated respectively in Figs. 2(a)-2(d). It is clear that the velocity boundary layer decreases along axial and transverse directions with rising values of λ. Also observed that the curvature raises between the regions $0 < \eta \le 0.0012$ (not exact determinate) and suddenly down within the region $-0.0061 < \eta \le 0.0012$ (not exact determinate) and then the curve strictly enhances in the region $-0.0061 < \eta \le 0$ along transverse direction. This means that the characteristics length between nanoparticle and swimming microorganisms are weakens in rotating bio-convection nanofluid flow. Further, S and ϕ profiles show decreasing behavior for increasing values of λ. The behavior of M on axial velocity is observed in Fig. 3. It is noticed that the raising values of M smoothly increases the axial velocity (f) within the region in presence and absence of viscous variation λ. This is due to the presence of temperature dependent viscosity. Moreover, the fluid has less velocity in case of $\lambda = 0$ when compared with $\lambda = 0.5$. Physically, temperature plays the dominant role in increasing the velocity profiles.

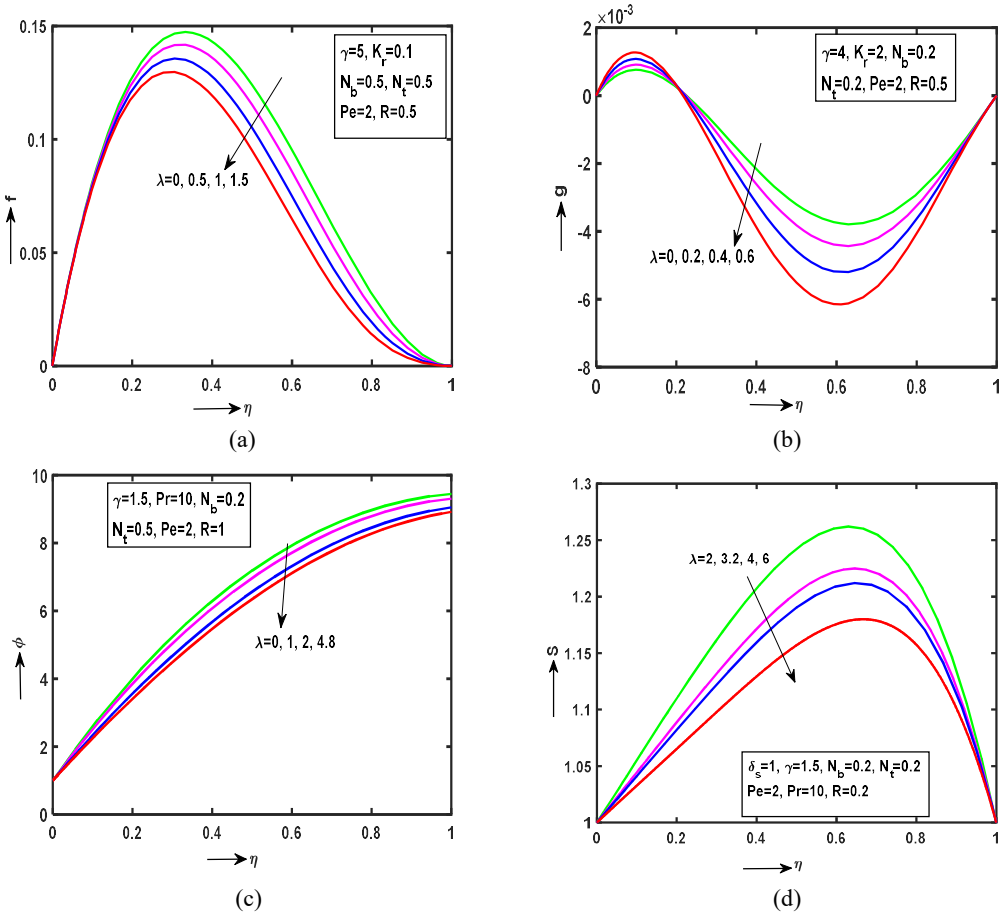

Fig. 2. (a) Behavior of λ on f, (b) behavior of λ on g, (c) behavior of λ on ϕ, (d) behavior of λ on S

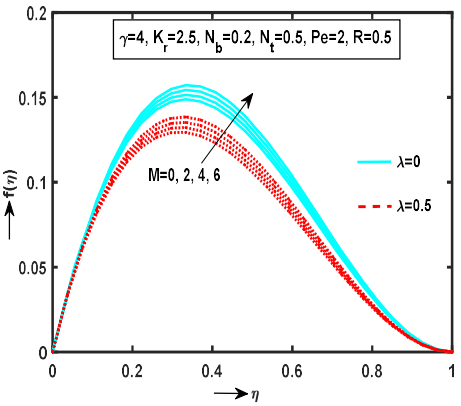

Fig. 3. Behavior of M on f

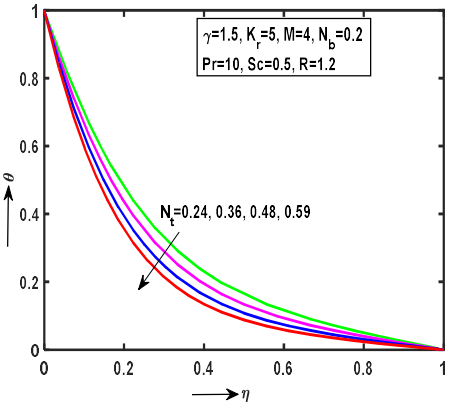

Fig. 4(a) Behavior of N_t on θ

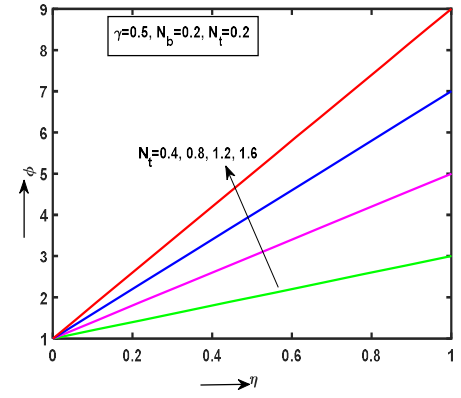

Fig. 4(b) Behavior of N_t on ϕ

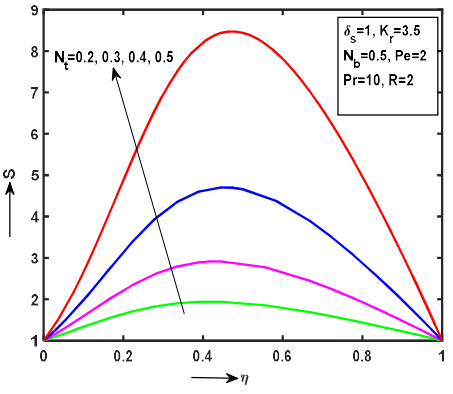

Fig. 4(c) Behavior of N_t on S

Figs. 4(a)-4(c) predict the influence of thermophoresis parameter N_t on θ, ϕ and S respectively. It is clear that the thermal boundary layer thickness smoothly declines and the behavior of ϕ and S increase for rising values of N_t. Physically, thermophoresis parameter is inversely proportional to the thermal conductivity α_m, and hence high thermal conductivity in nanoparticle and microorganisms' fluid flows are attained at upper rotation plate with higher values of N_t.

The effects of Brownian parameter N_b on θ, ϕ and S are illustrated respectively in Figs. 5(a)-5(c). It is noticed that θ, ϕ and S decrease for increasing values of N_b. Physically, the Brownian motion is inversely proportional to the thermal conductivity. Therefore, the high thermal conductivity produces low heat.

Figures 6(a)-6(c) explored the thermal radiation parameter R_d on θ, ϕ and S. It is observed that the temperature θ enhances with rising of R_d while reverse behavior observed in case of ϕ and S.

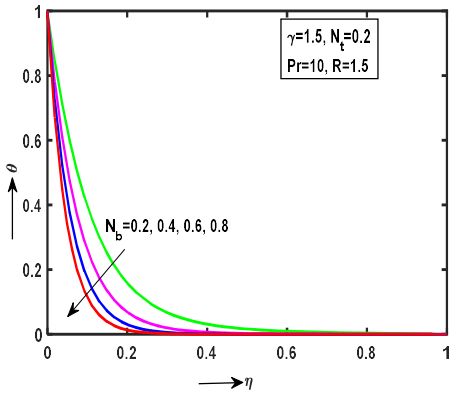

Fig. 5(a) Behavior of N_b on θ

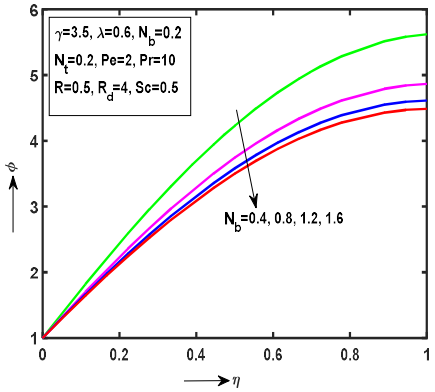

Fig. 5(b) Behavior of N_b on ϕ

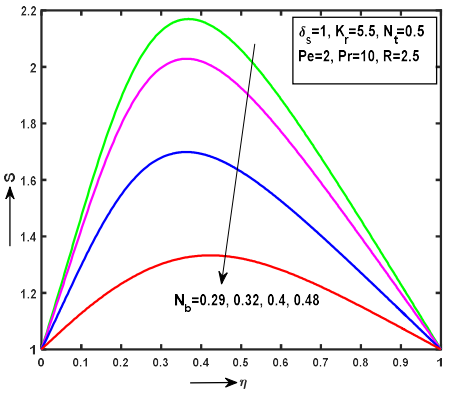

Fig. 5(c) Behavior of N_b on S

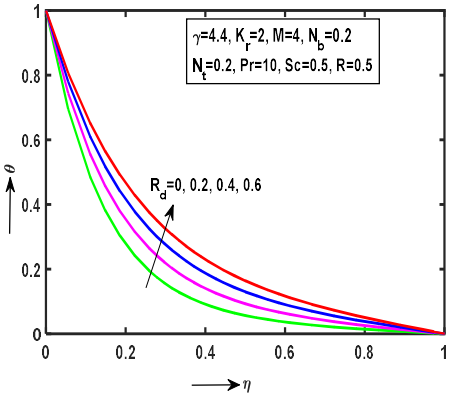

Fig. 6(a) Behavior of R_d on θ

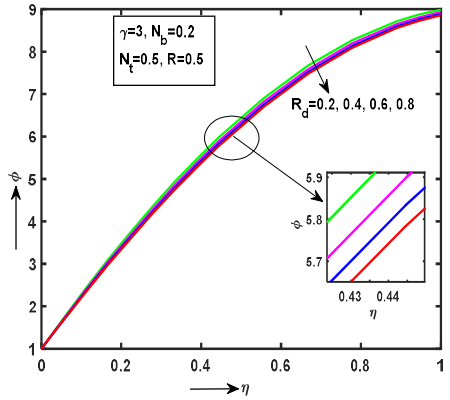

Fig. 6(b) Behavior of R_d on ϕ

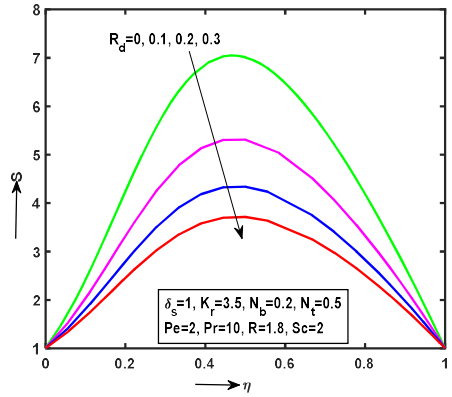

Fig. 6(c) Behavior of R_d on S

Figures 7(a)-7(f) represent the influence of particle concentration parameter R on f, g, θ, ϕ, S and Nu_x respectively. It is noticed that all of the velocities, temperature and rate of heat transfer decrease with rising values of R and opposite trend is observed in case of ϕ and S. Physically, larger values of R which strengthening the inertial forces and tend to reduce the

temperature field. Also, it is observed that the nanofluid axial velocity f approaches to the boundary value very fast in case of temperature dependent viscosity ($\lambda = 0.5$). Moreover, in case of transverse velocity the curve is smoothly raised between the region $0 < \eta \le 0.026$ (not exact determined) and suddenly decreased within the region $0.026 < \eta \le -0.3131$ (not exact determined), again the curve should be raised within $-0.3131 < \eta \le 0$. The oscillations of the velocity in due to the presence of temperature dependent viscosity.

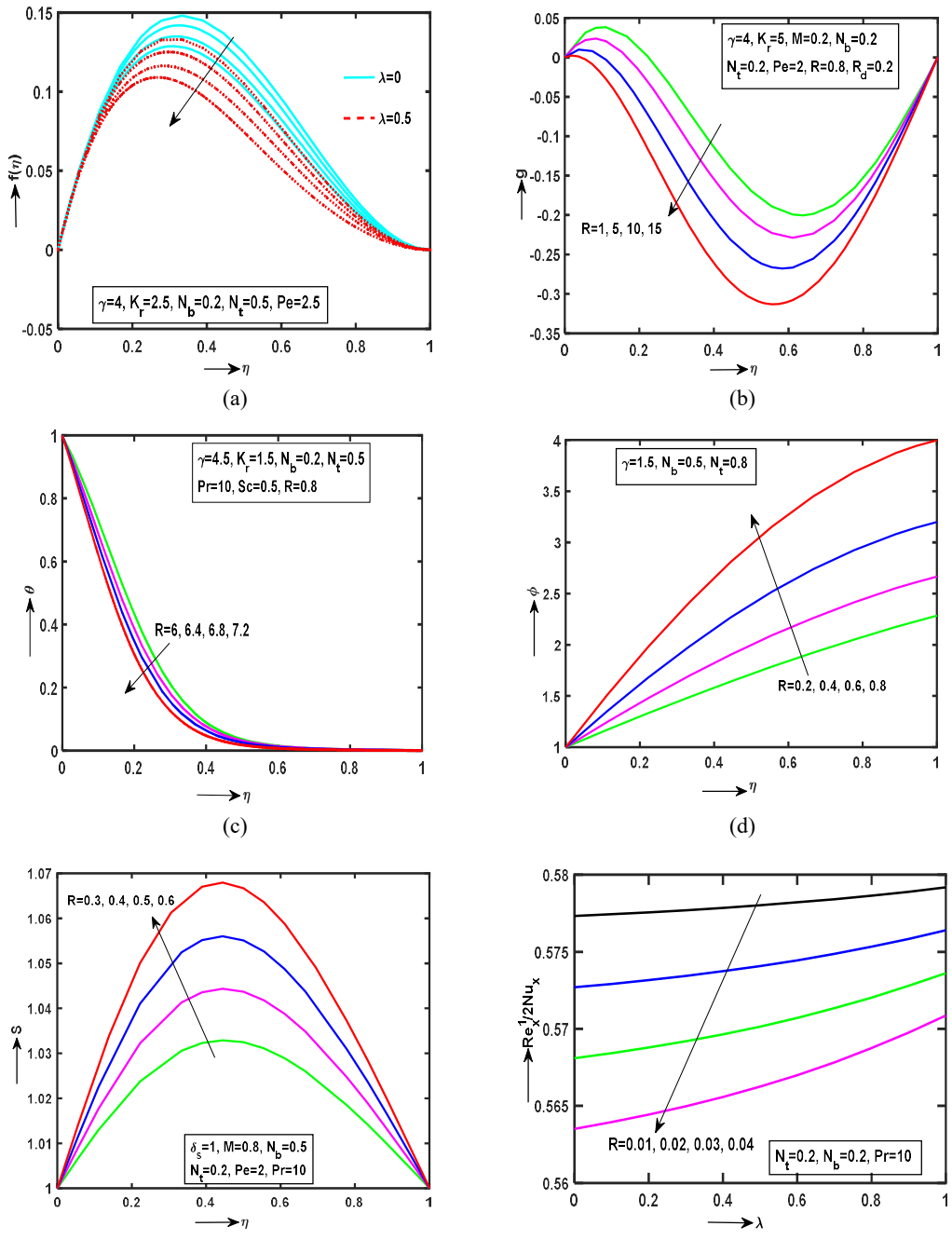

Fig. 7. Behavior of R on (a) f (b) g (c) θ (d) ϕ (e) S (f) $\mathrm{Re}_x^{-1/2} Nu_x$

Figs. 8(a)-8(d) discussed the rotational parameter K_r on f, g , S and Nu_x. The rotational parameter describes the interaction between bio-convection fluid density and dynamic viscosity at lower plate. It is clear that the flow directions on f and g are opposite for distinct values of K_r. This is due to the Carioles force which acts opposite to the transverse direction g. Also, it is noticed that the curve is smoothly increased within the area $0 < \eta \le 0.02735$ (not exact determined) and suddenly down within the region $0.02735 < \eta \le -0.1364$ (not exact determined), again the curve raises within the region $-0.1364 < \eta \le 0$ and finally approaches to the boundary. It is noticed that S increases and Nu_x decrease with rising values of K_r. Physically, K_r is interaction between bio-convection fluid density ρ_f and dynamic viscosity μ. Due to this reason at lower plate the dynamic viscosity of bio-convection fluid flow is low.

Figs. 9(a) and 9(b) illustrate the concentration profile and mass transfer rate for different values of γ (chemical reaction parameter). It is noticed that the concentration boundary layer strictly raises for increasing values of γ. Moreover, the mass transfer rate enhances in presence and absents of N_t, N_b against λ for certain values of γ. Physically, γ is proportional to dynamic viscosity μ_0. Due to this phenomenon the bioconvection fluid flow in rotating system at lower plate generates high mass transfer rate. Also the mass transfer rate is more in case of nanofluid flow than to the regular fluid ($N_t = N_b = 0$).

Figs. 10(a) and 10(b) represent the influence of Péclet number Pe on nanofluid bio-convection flow of S and Nu_x. It is observed that S increase and Nu_x decrease for rising values of Pe. The Pe is defined as the ratio between cell swimming speed W_c and variable microorganism diffusion D_n. Therefore, the swimming speed and dense of microorganisms is greater of bioconvection fluid flow in rotating plates.

Table 1. Comparison for numerical results of velocities $(f(\eta), g(\eta))$ with Din et al. [56] for different values of η when $\lambda = 0$

η	$f(\eta)$		$g(\eta)$	
	Ref. [56]	Present Study	Ref. [56]	Present Study
0.0	0.0000000	0.0000000000	-0.00000000	-0.00000000000
0.4	0.1396799	0.1396799105	-0.00200745	-0.00200745289
0.8	0.0307203	0.0307203278	-0.00269764	-0.00269764994
1.0	0.0000000	0.0000000000	-0.00000000	-0.00000000000

Fig. 11 discusses the behavior of Schmidt number Sc on mass transfer rate. It is noticed that the mass transfer rate smoothly down with rising values of Sc. Physically, the low kinematic viscosity of fluid in rotating plate generate low mass transfer rate in middle of rotating plates. Also, observed that the mass transfer rate for regular fluid is lower than that of nanofluid.

Table 1 is displayed to validate the present outcomes by comparing the axial and normal velocities $f(\eta)$, $g(\eta)$ of the fluid with those of Ref. [56] in a limiting sense ($\lambda = 0$). It is observed that the results of present limiting sense are very good agreement with the numerical values of Din et.al [56]. Table 2 represents the Nusselt number $\mathrm{Re}_x^{-1/2}\,\mathrm{Nu}_x$ with various parameters of R, K_r, γ, Pe, M, *and* Sc for $\lambda = 0$. We noticed that, the $\mathrm{Re}_x^{-1/2}\,\mathrm{Nu}_x$ deduces for distinct values of R, K_r, γ, and Pe while it enhanced for higher values of M, Sc.

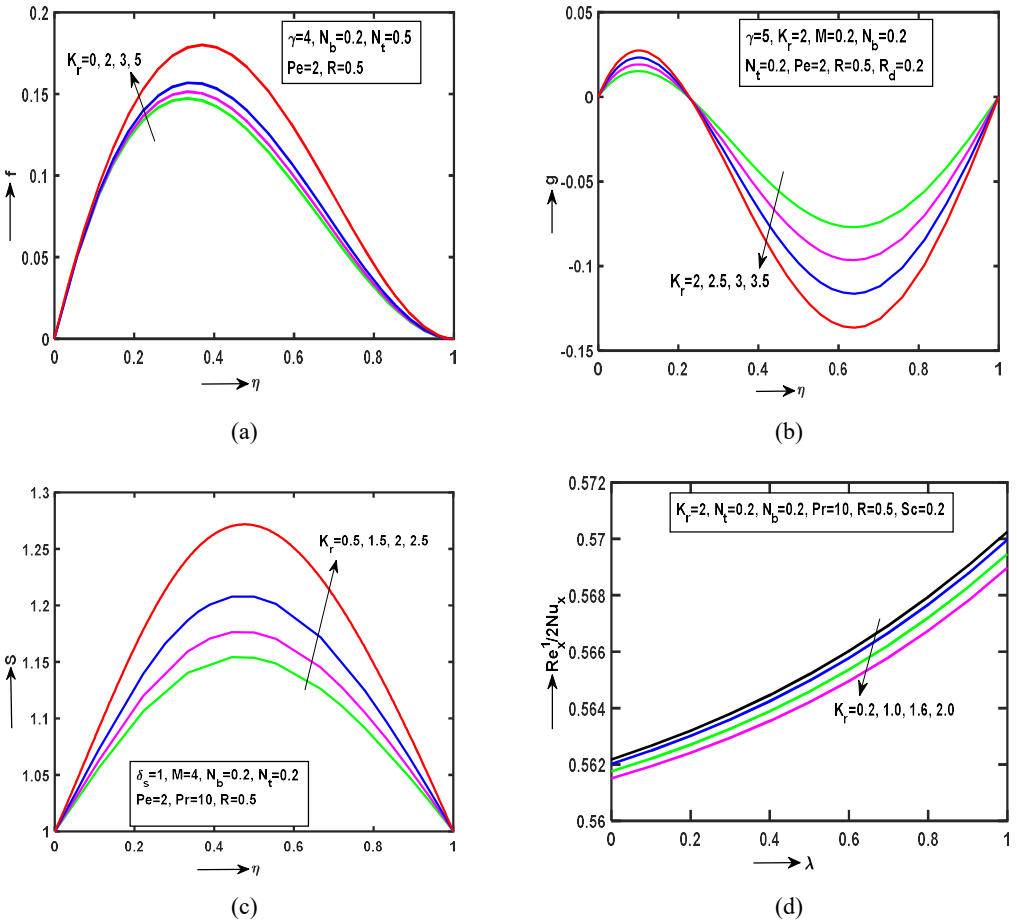

Fig. 8. Behavior of K_r on (a) f (b) g (c) S (d) $\mathrm{Re}_x^{-1/2}\,\mathrm{Nu}_x$

Table 2. Numerical values of Nu_x with different parameters of R, K_r, γ, Pe, M and Sc

R	K_r	γ	Pe	M	Sc	Nu_x
0.01						0.5635
0.02						0.5681
0.03						0.5727
0.04						0.5773
	0.2					0.5615
	1					0.5618
	1.6					0.5620
	2.0					0.5622
		0.15				0.3531
		0.2				0.3673
		0.25				0.3813
		0.30				0.3952
			0.01			0.5714
			0.02			0.5721
			0.03			0.5727
			0.04			0.5734
				0.15		-2.2740
				0.20		-2.3333
				0.25		-2.3910
				0.30		-2.4467
					0.1	0.4630
					0.2	0.4508
					0.3	0.4595
					0.4	0.4694

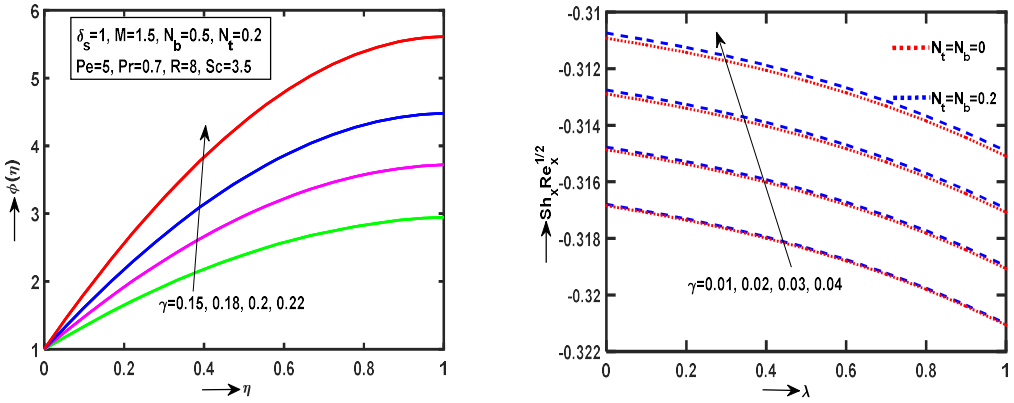

(a) (b)

Fig. 9. Behavior of γ on (a) ϕ and (b) $\mathrm{Re}_x^{1/2} Sh_x$

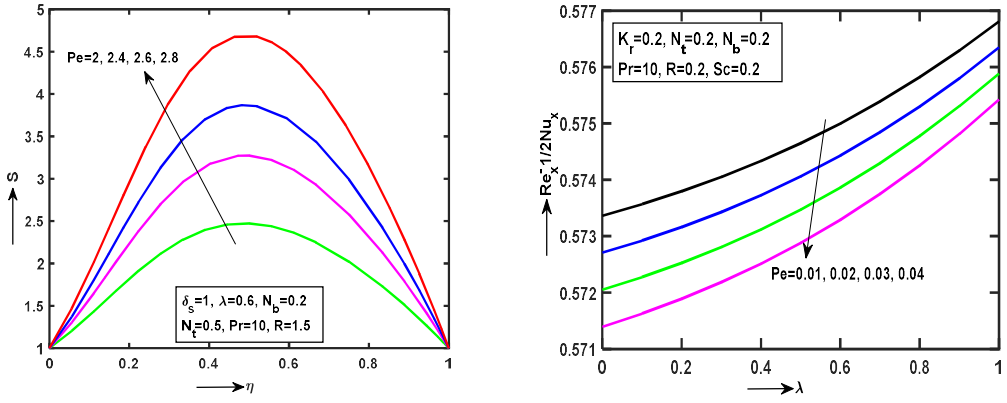

(a) (b)

Fig. 10. Behavior of Pe on (a) S and (b) $\mathrm{Re}_x^{-1/2} \mathrm{Nu}_x$

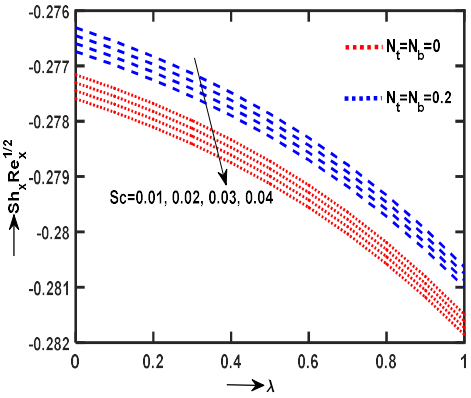

Fig. 11. Behavior of Sc on $\mathrm{Re}_x^{1/2} Sh_x$

4. Conclusion

The 3D bio-convection nanofluid flow containing gyrotactic microorganism in a rotating system with chemical reaction and thermal radiation is analyzed. The 4th order RKF MATLAB programming procedure is used for solving the coupled non-linear equations. Impact of different physical parameters on the fluid flow field are discussed and shown in figures. The main outcomes of this work are listed below.

- The concentration of bioconvection fluid flow strictly increases with rising values of γ .
- The mass transfer rate has opposite effect with γ and Sc .
- Mass transfer rate is more in case of nanofluid than to the regular fluid.
- The effect of R on temperature and motile density is reverse.
- Motile density distribution decreases by increasing Rd and Nb.
- Enhancement of the concentration for larger N_t and R.

Nomenclature

A, B, C :Velocity Components along x, y, z
(x, y): Cartesian coordinate's
(u, v): Velocity components along x, y
Ψ : Nanoparticle volume fraction
c_f : Skin friction coefficient
c_0: Nanoparticle volume fraction on lower wall
D_n: Variable microorganism diffusion coefficient
D_0: Brownian diffusion
D_Θ : Thermophoresis diffusion
f: Dimensionless stream function
f': Dimensionless velocity
f_w: Section parameter
k^*: Mean absorption coefficient
K_r: Rotational parameter
Le: Lewis number
M: Magnetic parameter
N: Number of motile microorganisms
N_h: Lower wall motile microorganisms
N_0: Upper wall motile microorganisms
N_b: Brownian motion coefficient
N_t: Yhermophoresis parameter

Θ : Fluid temperature
Θ_0, Θ_h : Temperature on lower, upper wall
A_∞ : Free stream velocity
A_W : Stretching velocity
W_c : Maximum cell swimming speed

Greek symbols

θ: Dimensionless temperature
ϕ : Dimensionless concentration
α : Wall expansion ratio
σ : Electrical conductivity
α_m : Thermal conductivity
γ: Chemical reaction parameter
σ^*, k^* : Boltzmann constant
μ_{nf} : Dynamic viscosity of nanofluid
υ : Kinematic viscosity
λ : Viscosity variation parameter
μ_0 : Dynamic viscosity at lower plate
τ_w : Wall shear stress
ρ_{nf} : Density of nanofluid
δ_s : Constant
ρ_s : Density of the solid

Nu_x: Nusselt number

Pr: Prandtl number

P*e*: Bio convection Péclet number

Pr: Prandtl number

q_n: Surface microorganism flux

q_r: Radiative heat flux

R_d: Radiation parameter

R: Viscosity parameter

Re_x: Reynolds number

Sc: Schmidt number

S: Wall mass transfer parameter

ρ_f : Fluid density

$\left(\rho c_p\right)_f$: Heat capacity of the field

$\left(\rho c_p\right)_p$: Heat capacity of the nanoparticle material

τ : Parameter defined by

η: Similarity variable

ψ : Stream function

Ω : Constant rotational velocity

ρ : Fluid density

Subscripts

∞ : Condition at free stream

w: Wall mass transfer velocity

Conflict of Interest

The author(s) declared no potential conflicts of interest with respect to the research, authorship and publication of this article.

Funding

The author(s) received no financial support for the research, authorship and publication of this article.

References

[1] Choi, S.U.S., Eastman, J. A., Enhancing thermal conductivity of fluids with nanoparticles, Developments and Applications of Non-Newtonian Flows, *ASME MD* 231, 1995, 99-105.

[2] Das, K., Duari, P.R., Kundu, P.K., Nanofluid bioconvection in presence of gyrotactic microorganisms and chemical reaction in a porous medium, *J. Mech. Sci. Tech.,* 29(11), 2015, 4841-4849.

[3] Khan, U., Ahmed, N., Din, S.T.M., Influence of viscous dissipation and joule heating on MHD bio-convection flow over a porous wedge in the presence of nanoparticles and gyrotactic microorganisms. *Springer plus*, 5, 2016, 1-18.

[4] Childress, S., Levandowsky, M., Spiegel, E.A., Pattern formation in a suspension of swimming micro-organisms: equations and stability theory. *J. Fluid Mech.* 69, 1975, 591-613.

[5] Hill, N.A., Pedley, T.J., Kessler, J.O., Growth of bio convection patterns in a suspension of gyrotactic microorganisms in a layer of finite depth, *J. Fluid Mech.* 208, 1989, 509-543.

[6] Kuznetsov, A.V., Nanofluid bioconvection in water-based suspensions containing nanoparticles and oxytactic microorganisms: oscillatory instability, Nanoscale Res. Lett., 6(100), 2011, 1-13.

[7] Xinyu, W., Huiying, W., Cheng, P., Pressure drop and heat transfer of al_2o_3-h_2o nanofluids through silicon Microchannels, *J. Micro. Mech. Micro. Eng.,* 19, 2009, 105020(11).

[8] Xu, H., Pop, I., Fully developed mixed convection flow in a horizontal channel filled by a nanofluid containing both nanoparticles and gyrotactic microorganisms, *European J. Mech. B/Fluids*, 46, 2014, 37-45.

[9] Uddin, M.J., Alginahi, Y., Bég, O.A., Kabir, M.N., Numerical solutions for gyrotactic bioconvection in nanofluid-saturated porous media with Stefan blowing and multiple slip effects, *Comp. Math. Appl.,* 72, 2016, 2562-2581.

[10] Siddiqa, S., Hina, G.E., Begum, N., Saleem, S., Hossain, M.A., Rama Subba Reddy, G., Numerical solutions of nanofluid bioconvection due to gyrotactic microorganisms along a vertical wavy cone, *Int. J. Heat Mass Transfer,* 101, 2016, 608-613.

[11] Mohsin, B.B., Ahmed, N., Adnan, Khan, U., Din, S.T.M., A bioconvection model for a squeezing flow of nanofluid between parallel plates in the presence of gyrotactic microorganisms, *Eur. Phys. J. Plus.,* 132(187), 2017, 1-12.

[12] Iqbal, Z., Mehmood, Z., Azhar, E., Maraj, E.N., Numerical investigation of Nanofluidic transport of gyrotactic microorganisms submerged in water towards Riga plate, *J. Mole. Liq.,* 234, 2017, 296-308.

[13] Ojjela, O., Ramesh, K., Das, S.K., Second Law Analysis of MHD Squeezing Flow of Casson Fluid between Two Parallel Disks, *Int. J. Chemical. Reactor Eng.,* 6(16), 2018, https://doi.org/10.1515/ijcre-2017-0163.

[14] Li, Z., Sheikholeslami, M., Chamkha, A.J., Raizah, Z.A., Saleem, S., Control volume finite element method for nanofluid MHD natural convective flow inside a sinusoidal annulus under the impact of thermal radiation, *Comp. Methods Appl. Mech. Eng.,* 338(15), 2018, 618-633.

[15] Mahian, O., Kolsi, L., Amani, M., Estelle, P., Ahmadi, G., Kleinstreuer, C., Marshall, J.S., Taylor, R.A., Nada, E.A., Rashidi, S., Niazmand, H., Wongwises, S., Hayat, T., Kasaeian, A., Pop, I., Recent advances in modeling and simulation of nanofluid flows-part II: *Applications Physics Reports,* 791, 2019, 1-59.

[16] Li, Z., Shehzad, S.A., Sheikholeslami, M., An application of CVFEM for nanofluid heat transfer intensification in a porous sinusoidal cavity considering thermal non-equilibrium model, *Comp. Meth. Appl. Mech. Eng.,* 339(1), 2018, 663-680.

[17] Mahian, O., Kolsi, L., Amani, M., Estelle, P., Ahmadi, G., Kleinstreuer, C., Marshall, J.S., Siavashi, M., Taylor, R.A., Niazmand, H., Wongwises, S., Hayat, T., Kolanjiyil, A., Kasaeian, A., Pop, I., Recent advances in modeling and simulation of nanofluid flows-Part I: Fundamental and theory, *Physics Reports,* 790, 2019, 1-48.
[18] Mahian, O., Kianifar, A., Kalogirou, S.A., Pop, I., Wongwises, S., A review of the applications of nanofluids in solar energy, *Int. J. Heat Mass Transfer* 57, 2013, 582-594.
[19] Mahian, O., Pop, I., Sahin, A.Z., Oztop, H.F., Wongwises, S., Irreversibility analysis of a vertical annulus using TiO_2/water nanofluid with MHD flow effects, *Int. J. Heat Mass Transfer* 64, 2013, 671-679.
[20] Mahian, O., Kleinstreuer, C., Nimr, M.A.A., Pop, I., Wongwises, S., A review of entropy generation in nanofluid flow, *Int. J. Heat Mass Transfer* 65, 2013, 514-532.
[21] Naseem, F., Shafiq, A., Zhao, L., Naseem, A., MHD bio convective flow of Powell eyring nanofluid over stretched surface, *AIP Advances,* 7, 2017, 1-21.
[22] Chakraborty, T., Das, K., Kundu, P.K., Framing the impact of external magnetic field on bioconvection of a nanofluid flow containing gyrotactic microorganisms with convective boundary conditions, *Alexandria Eng. J.,* 2016, 1-11.
[23] Alsaedi, A. Khan, M.I., Farooq, M., Gull, N., Hayat, T., Magnetohydrodynamic stratified bio convective flow of nanofluid due to gyrotactic microorganisms, *Advanced Powder Tech.* 28, 2017, 288-298.
[24] Acharya, N., Das, K., Kundu, P.K., Framing the effects of solar radiation on magneto-hydrodynamics bioconvection nanofluid flow in presence of gyrotactic microorganisms, *J. Mole. Liq.*, 222, 2016, 28-37.
[25] Sheikholeslami, M., Ganji, D.D., Javed, M.Y., Ellahi, R., Effect of Thermal Radiation on Magnetohydrodynamics Nanofluid flow and Heat Transfer by Means of two Phase Model, *J. Magne. Magn. Mater,* 374, 2017, 36-43.
[26] Hsiao, K.L., Micropolar nanofluid flow with MHD and viscous dissipation effects towards a stretching sheet with multimedia feature, *Int. J. Heat Mass Transfer*, 112, 2017, 983-990.
[27] Tamoor, M., Waqas, M., Khan, M.I., Alsaedi, A., Hayat, T., Magnetohydrodynamic flow of casson fluid over a stretching cylinder, *Results Phys,* 3, 2017, 1-5.
[28] Ramzan, M., Bilal, M., Chung, J.D., Mann, A.B., On MHD radiative Jeffery nanofluid flow with convective heat and mass boundary conditions, *Neural Comp. Appl.,* 9, 2017, 2739-2748.
[29] Tekade, S.P., Shende, D.Z., Wasewar, K.L., Hydrogen Generation in an Annular Micro-Reactor: An Experimental Investigation and Reaction Modelling by Shrinking Core Model (SCM), *Int. J. Chemical Reactor Eng.,* 7(16), 2018. DOI: https://doi.org/10.1515/ijcre-2017-0202.
[30] Siddiqa, S., Faryad, A., Begum, A., Hossain, M.A., Rama Subba Reddy, G., Periodic magnetohydrodynamic natural convection flow of a micropolar fluid with radiation, *Int. J. Thermal Sci.,* 111, 2017, 215-222.
[31] Khan, M., Malik, M.Y., Salahuddin, T., Rehman, K.U., Naseer, M., Khan, I., MHD flow of Williamson nanofluid over a cone and plate with chemically reactive species, *J. Mole. Liq.,* 231, 2017, 580-588.
[32] Devika, B., Satya Narayana, P.V., Venkataramana, S., MHD oscillatory flow of a viscoelastic fluid in a porous channel with chemical reaction, *Int. J. Eng. Science Invention*, 2(2), 2013, 26-35.
[33] Jena, S., Mishra, S.R., Dash, G.C., Chemical reaction effect on MHD Jeffery fluid flow over a stretching sheet through porous media with heat generation/absorption, *Int. J. Appl. Comp. Math.,* 2, 2016, 1225-1238.
[34] Javaid, S., Aziz, A., Influence of variable thermal conductivity and thermal radiation on slip flow and heat transfer of MHD power-law fluid over a porous sheet, *Thermal Sci.* 2016, 65-65.
[35] Satya Narayana, P.V., Venkateswarlu, B., Devika, B., Chemical reaction and heat source effects on MHD oscillatory flow in an irregular channel, *Ain Shams Eng. J.* 2016, 1079-1088.
[36] Hayat, T., Rashid, M., Imtiaz, M., Alsaedi, A., MHD convective flow due to a curved surface with thermal radiation and chemical reaction, *J. Mole. Liq.,* 225, 2017, 482-489.
[37] Xun, S., Zhao, J., Zheng, L., Zhang, X., Bioconvection in rotating system immersed in nanofluid with temperature dependent viscosity and thermal conductivity, *Int. J. Heat Mass Transfer,* 111, 2017, 1001-1006.
[38] Sheikholeslami, M., Ganji, D.D., Numerical investigation for two phase modeling of nanofluid in a rotating system with permeable sheet, *J. Mole. Liq.,* 194, 2014, 13-19.
[39] Sheikholeslami, M., Ganji, D.D., Three dimensional heat and mass transfer in a rotating system using nanofluid, *Powder Tech.,* 253, 2014, 789-796.
[40] Mustafa, M., Khan, J.A., Numerical study of partial slip effects on MHD flow of nanofluids near a convectively heated stretchable rotating disk, *J. Mole. Liq.,* 234, 2017, 287-295.
[41] Makinde, O.D., Mabood, F., Khan, W.A., Tshehla, M.S., MHD flow of a variable viscosity nanofluid over a radially stretching convective surface with radiative heat, *J. Mole. Liq.,* 219, 2016, 624-630.
[42] Sheikholeslami, M., Ganji, D.D., Impact of electric field on nanofluid forced convection heat transfer with considering variable properties, *J. Mole. Liq.,* 229, 2017, 566-573.
[43] Chen., X, Hu., Z, Lei Zhang., L, Zhen Yao., Z, Chen., X, Zheng., Y, Liu., Y, Wang., Q, Yang Liu., Y, Cui., X, Song., H., Numerical and Experimental Study on a Microfluidic Concentration Gradient Generator for Arbitrary Approximate Linear and Quadratic Concentration Curve Output, *Int. J. Chemical. Reactor Eng.,* 1(16), 2018. doi: 10.1515/ijcre-2016-0204.
[44] Sheikholeslami, M., Ganji, D.D., Numerical investigation for two phase modeling of nanofluid in a rotating system with permeable sheet, *J. Mole. Liq.,* 194, 2014, 13-19.
[45] Kumar, R., Sood, S., Shehzad, S.A., Sheikholeslami, M., Radiative heat transfer study for flow of non-Newtonian nanofluid past a Riga plate with variable thickness, *J. Mole. Liq.,* 248, 2017, 43-152.

[46] Nield, D.A., Kuznetsov, A.V., Thermal instability in a porous medium layer saturated by a nanofluid, *Int. J. Heat Mass Transfer,* 52, 2009, 5796-5801.
[47] Kuznetsov, A.V., Non-oscillatory and oscillatory nanofluid bio-thermal convection in a horizontal layer of finite depth, *European J. Mech. B/Fluids*, 30, 2017, 156-165.
[48] Sheikholeslami, M., Ganji, D.D. Javed, M.Y. Ellahi, R., Effect of thermal radiation on Magnetohydrodynamics nanofluid flow and heat transfer by means of two phase model, *J. Magn. Magnet. Mater.* 374, 2017, 36-43.
[49] Attia, H.A., Kotb, N.A., MHD flow between two parallel plates with heat transfer, *Acta Mech.,* 117, 1996, 1257-1266.
[50] Attia, H.A., Transient MHD flow and heat transfer between two parallel plates with temperature dependence viscosity, *Mech. Res. Comm.,* 26, 1999, 115-121.
[41] Attia, H.A., Cairo, Egypt, Influence of temperature dependence viscosity on the MHD-channel flow of dusty fluid with heat transfer, *Act Mach.,* 151, 2001, 89-101.
[52] Attia, H.A., MHD couette flow with temperature dependent viscosity and the ion slip, *Tamkang J. Sci. Eng.,* 8(1), 2005, 11-16.
[53] Lai, F., Kulacki, F., The effect of variable viscosity on convective heat transfer along a vertical surface in a saturated porous medium, *Int. J. Heat Mass Transfer,* 33(5), 1990, 1028–31.
[54] Devi, S.P.A., Prakash, M., Temperature dependent viscosity and thermal conductivity effects on hydromagnetic flow over a slendering stretching sheet, *J. Nigerian Math. Society,* 34, 2015, 318-330.
[55] Brewster, M.Q., *Thermal Radiative Transfer Properties,* Wiley, New York, 1992.
[56] Din, S.T.M., Zaidi, Z.A., Khan, U., Ahmed, N., On heat and mass transfer analysis for the flow of a nanofluid between rotating parallel plates, *Aerospace Sci. Tech.*, 46, 2015, 514-522.